A COMBINATION OF EMD AND VARMA MODEL FOR STRUCTURAL DAMAGE DETECTION

Y.F. Dong[1] and Y.M. Li[2]

[1] *Instructor, College of Civil Engineering, Chongqing University, Chongqing, China*
Email: dongyinfeng@cqu.edu.cn

[2] *Professor, College of Civil Engineering, Chongqing University, Chongqing, China;*
Key Laboratory of New Technique for Construction of Cities in Mountain Area, Chongqing University, Chongqing, China
Email: liyingmin@cqu.edu.cn

ABSTRACT :

A method combining the empirical mode decomposition (EMD) and vector autoregressive moving average (VARMA) model is proposed to detect the damage of structures. First, the EMD method is used to decompose the dynamic response of structures into a set of intrinsic mode functions (IMFs). Then, these IMFs are represented as a time varying VARMA model and Kalman filter is used to estimate the corresponding time varying VARMA coefficients. Finally, a novel index, derived from the time varying VARMA parameters, is proposed to identifying the damage of structures. The acceleration response recorded at a 6-story reinforced concrete building, the Imperial County Services Building, during the 1979 Imperial Valley earthquake, is analyzed to demonstrate the efficiency of the proposed method. It is found that the proposed method can precisely indicate the damage and changes of dynamic properties of structures, which is expected as the promising area for future research.

KEYWORDS: damage detection, dynamic response, EMD, VARMA model

1. INTRODUCTION

Structural damage detection is an important and challenging problem in earthquake engineering. As a systemic research field, it involves the intersection and integration of various disciplines such as signal processing, stochastic process theory, structural dynamic analysis, system identification, sensor technology, and numerical simulation. The major purpose of structural damage detection is to identify the occurrence (presence), location and type of damage, quantify the damage severity, and predict the remaining service life of the structure. The vibration signals measured from the instrumented structure are often used for this purpose.

Since last three decades, a lot of damage detection methods have been developed. Excellent review work on this topic can be found in (Sohn 2003 and Chang 2003). The commonly used damage detection methods can be roughly divided into two categories. One is the method that estimates the physical parameters such as stiffness or damping ratios directly and investigates their changes. The other mainly consists of various vibration-based methods that monitor changes in the modal properties of the structures (modal frequencies, mode shapes and modal damping). The basic premise of these methods is that modal parameters are a function of the physical properties of the structure (mass, damping, stiffness, and boundary conditions). Therefore, changes in physical parameters of the structure will cause changes in modal properties. For modal parameters are in many cases easier to evaluate in the field than physical parameters, this category is more attractive. However, the effectiveness of this category is usually limited by configuration of sensors, parameter estimation error, measurement noise, and sensitivity of modal parameters to structural damage. Continuous efforts to reduce such limitations have given rise to some improved methods. In addition, some more recent research also indicated that using proper methods to extract physically meaningful information from vibration signals and detecting structural damage by use of novelty analysis may be a new trend. This undoubtedly requires an efficient method for processing vibration signals, which are often nonlinear and nonstationary in nature.

As a breakthrough to conventional signal processing methods, the Hilbert-Huang transform (HHT), developed by Huang (1998), is thought to be particularly suitable for processing nonlinear and nonstationary signals. HHT consists of empirical mode decomposition (EMD) and Hilbert spectral analysis (HSA). Though the efficiency of HHT has been demonstrated in considerable researches, there still exist at least two limitations associated with the restriction of Nuttall theorem and larger covariance (poorer frequency resolution and readability) of the Hilbert spectrum at higher frequencies (Dong 2008). To address above problems, in Dong (2008) a time varying vector autoregressive moving average (VARMA) model based method was proposed to calculate the instantaneous frequencies of IMFs and yield the Hilbert spectrum. Preliminary results showed the method was quite effective.

In this study, we propose a novelty index derived from the time varying VARMA coefficients to detect the structural damage as a further application of the improved HHT method. For the novelty index is defined based on the feature extraction of a vibration signal and no additional modal information is required, it can be used to detect both global and local structural damages. Another merit of the novelty index is that it can be potentially used for real time (online) structural damage detection, for it is derived from time varying VARMA coefficients. In the example given, the Imperial County Services Building (Todorovska 2007 and 2008) are used as testbed to explore the efficiency of the proposed novelty index. The recorded seismic responses are analyzed using both the improved and the original HHT methods, and the proposed novelty index is applied to detect the structural damages. The results demonstrate that the novelty index can indicate the occurrence and relative severity of structural damages at various locations in an efficient manner. Lastly, some recommendations for future research are provided.

2. THE IMPROVED HHT METHOD

The improved method, based on a time varying VARMA model, is summarized as follows (Dong 2008):
1. Perform the EMD process to get all the n IMFs from a given signal $x(k)$, which is the same as the original HHT method.
2. Represent the n IMFs as a time varying VARMA (p, q) model

$$\mathbf{y}(k) = \sum_{i=1}^{p} \mathbf{\Phi}_i(k)\mathbf{y}(k-i) + \sum_{i=1}^{q} \mathbf{\Theta}_i(k)\mathbf{u}(k-i) + \mathbf{u}(k) \tag{2.1}$$

where the vector $\mathbf{y}(k)$ consists of the n IMFs, i.e. $\mathbf{y}(k) = [c_1(k), c_2(k), \mathbf{L}, c_n(k)]^T{}_{n\times 1}$ and $c_i(k)$ is the ith IMF. The autoregressive coefficients $\mathbf{\Phi}_i(k)$ and the moving average coefficients $\mathbf{\Theta}_i(k)$ are $n\times n$ matrices. The vector $\mathbf{u}(k)$ is an n-dimensional zero-mean Gaussian white noise process with covariance matrix $R(k)\cdot\mathbf{I}$, where $\mathbf{I}$ is the unit matrix and $R(k) > 0$. The variable k indicates the time instant $t = k\cdot\Delta t$ with Δt as the sampling interval. It has been shown by Pandit (1991) and Anderson (1997) that a time varying n-dimensional VARMA (2m, 2m-1) model is equivalent to a time varying system with nm degrees of freedom (DOF). For all the n IMFs are orthogonal monocomponent signals, they can be viewed as the n outputs of a time varying n-DOF system, and the n instantaneous eigenfrequencies (natural frequencies) of the system can be designated as the instantaneous frequencies of the IMFs. Consequently, a time varying n-dimensional VARMA (2, 1) model can be used to represent the n IMFs.
3. Recast the time varying VARMA (p, q) model into state space form

$$\begin{cases} \xi(k) = \xi(k-1) + \mathbf{v}(k-1) \\ \mathbf{y}(k) = [\mathbf{H}(k)\xi(k)]^T + \mathbf{u}(k) \end{cases} \tag{2.2}$$

where $\xi(k) = [\mathbf{\Phi}_1(k), \mathbf{L}, \mathbf{\Phi}_p(k), \mathbf{\Theta}_1(k), \mathbf{L}, \mathbf{\Theta}_q(k)]^T$ is called state vector. $\mathbf{v}(k) = [\mathbf{v}_1(k), \mathbf{v}_2(k), \mathbf{L}, \mathbf{v}_{p+q}(k)]^T$ is

Gaussian process noise with mean and covariance as $\mathbf{0}$ and $\mathbf{Q}(k)$ respectively where $\mathbf{Q}(k)$ is an symmetric positive definite matrix. $\mathbf{H}(k)=[\mathbf{y}(k-1)^T,\cdots,\mathbf{y}(k-p)^T,\mathbf{u}(k-1)^T,\cdots,\mathbf{u}(k-q)^T]$ is called measurement vector.
4. Use the Kalman filter to estimate $\xi(k)$ based on above state space model. For more details about the improved method and the algorithm of Kalman filter, the readers can refer to (Dong 2006 and 2008, Ljung 1999).
5. Define the system matrix $\mathbf{A}(k)$ as

$$\mathbf{A}(k)=\begin{bmatrix} \mathbf{\Phi}_1(k) & \mathbf{\Phi}_2(k) & \cdots & \mathbf{\Phi}_p(k) \\ \mathbf{I} & \mathbf{0} & \cdots & \mathbf{0} \\ \mathbf{0} & \mathbf{I} & & \mathbf{0} \\ \vdots & \vdots & & \vdots \\ \mathbf{0} & \cdots & \mathbf{I} & \mathbf{0} \end{bmatrix} \tag{2.3}$$

and decompose $\mathbf{A}(k)$ by taking eigenvalue decomposition

$$\mathbf{A}(k)=\mathbf{\Psi}(k)\boldsymbol{\lambda}(k)\mathbf{\Psi}(k)^{-1} \tag{2.4}$$

where $\boldsymbol{\lambda}(k)=diag[\lambda_i(k)]$ for $i=1, 2, \cdots, np$. Then, the instantaneous eigenfrequencies are given as

$$f_i(k)=\left\|\ln[\lambda_i(k)]\right\|/2\pi\Delta t \tag{2.5}$$

Because the instantaneous eigenvalues $\lambda_i(k)$ appear in complex conjugate pairs, one pair for each degree of freedom, we can get n different instantaneous eigenfrequencies when $p=2$, i.e. the instantaneous frequencies of the n IMFs.
6. For each IMF, define the envelope by a cubic spline through all the maxima. Then use all the envelopes and instantaneous frequencies to obtain the Hilbert spectrum.

3. THE NOVELTY INDEX

As has been described above, if an n-dimensional VARMA (2, 1) model is used in Eqn. 2.1 to represent $\mathbf{y}(k)$ as the n outputs of an n-DOF system to input $\mathbf{u}(k)$, the n different eigenvalue pairs in Eqn. 2.4 would yield n different mode frequencies of the system. In addition, the last n components of the eigenvectors $\mathbf{\Psi}(k)$ in Eqn. 2.4 would yield the mode shapes of the system. Similar to eigenvalues $\boldsymbol{\lambda}(k)$, eigenvectors $\mathbf{\Psi}(k)$ appear in complex conjugate pairs, one pair for each degree of freedom, thus we can get n different mode shapes of the system. Here, the time varying VARMA (2, 1) model is used to represent all the n IMFs of a given signal $x(k)$ as the outputs of a time varying system to white noise inputs and $x(k)$ is taken as the sum of the n IMFs and the residue. So the last n components of eigenvector $\mathbf{\Psi}_i(k)$ corresponding to eigenvalue $\lambda_i(k)$, i.e. the ith mode shape, can reveal physically meaningful information about the relative contribution of each IMF component to the global energy distribution of $x(k)$ in the frequency band around $f_i(k)$ each moment. Therefore, a novelty indicator $\mathbf{N}(k)=\{N_i(k), i=1,2,\cdots,n\}$ can be defined for the n IMFs to quantify their relative contributions to the global energy distribution and indicate the occurrence and relative severity of structural damage. The item $N_i(k)$ corresponding to the ith IMF component is given by

$$N_i(k)=\left\|y_{n+i,1}(k)\right\| \Big/ \sum_{j=n+1}^{2n}\left\|y_{j,1}(k)\right\| \tag{3.1}$$

where $y_{j,1}(k)$ is the jth component of the eigenvector $\mathbf{\Psi}_1(k)$. Here we only use the last n components of $\mathbf{\Psi}_1(k)$ to define the novelty indicator $\mathbf{N}(k)$, because the modulus of $l_1(k)$ is the largest and $\mathbf{\Psi}_1(k)$ is most sensitive to the change of system matrix $\mathbf{A}(k)$. Another reason is the same as the one discussed in Todorovska (2007 and 2008) that the novelty index is used to quantify the contribution of each IMF to the global energy distribution of $x(k)$ in the high frequency band around $f_1(k)$ which is away from the frequencies of the first few modes of typical buildings. And the abrupt changes in structural response $x(k)$ caused by sudden loss of stiffness due to structural damages can be detected in this high frequency band. These abrupt changes can be interpreted as sharp increase or decrease in $\mathbf{N}(k)$. Furthermore, this treatment can also help to eliminate the effects of soil-structure interaction which usually affect the low frequency part of structural response.

It is pointed out in Flandrin (2004) that EMD is equivalent to a dyadic filter bank and the characteristic scales of IMFs are designated to increase from the smallest to the largest. When structural damage occurs, the downward shift of signal energy from high frequency to low frequency due to structural damage will cause significant decrease in the contribution of small scale IMFs and significant increase in the contribution of large scale IMFs to the global energy distribution at high frequency. As $\mathbf{N}(k)$ is defined in the high frequency band around $f_1(k)$, in such cases, the item $N_1(k)$ corresponding to $c_1(k)$, i.e. the relative contribution of the IMF with the smallest characteristic scale, will decrease sharply and the other items in $\mathbf{N}(k)$ will increase simultaneously. When no structural damage occurs, all the items in $\mathbf{N}(k)$ will keep even, for the relative contribution of each IMF will not change with time.

4. RESULTS AND DISCUSSIONS

In this study, the Imperial County Services Building (Todorovska 2007 and 2008) is used as testbed to survey the efficiency of the proposed novelty index with actual noise. The recorded acceleration responses of this building during the 1979 Imperial Valley earthquake are analyzed using the improved and the original HHT methods, then the corresponding novelty indices are used to detect the structural damages. In addition, the results of short-time Fourier transform (STFT) and continuous wavelet transform (WT) are also provided to survey the variations in time-frequency properties of structural responses caused by structural damages and the performance of various signal processing methods. The Hanning window of length 128 points is used in STFT method and the Morlet wavelet is used in WT method. Here, only the novelty indicators for the first 5 IMF components are presented for simplicity, because the first 5 IMF components carry the majority of the signal energy in most cases.

The former Imperial County Services Building was a 6-story reinforced concrete building. It was severely damaged by the 1979 Imperial Valley earthquake and was later demolished. As has been reported in Todorovska (2007 and 2008), the major failure occurred in the columns at the east end of the building at the ground floor. The vertical reinforcement was exposed and buckled, and the core concrete could not be contained, which in turn caused the occurrence of damage on the 2nd, 3rd and higher floors. The sensor configuration of the recording system for this building is shown in Figure 1. To eliminate the effect of the nonlinearities in the response of the foundation soil, the relative angular accelerations are used. The relative angular acceleration $a_{i,j}$ is given by $a_{i,j}=(a_i - a_j)/d_{i,j}$ where a_i and a_j respectively denote the accelerations of sensors i and j with the separation distance as $d_{i,j}$. In this example, the relative angular accelerations $a_{4,5}$, $a_{5,6}$, and $a_{6,13}$ are used and the corresponding accelerograms are shown in Figure 2. For the energy of these relative angular accelerations mainly locate in the first 20s, only the portions for the first 20s are used for analysis.

Figures. 3 and 4 show the Hilbert spectra obtained using the improved as well as the original HHT methods, and the corresponding counterparts of the STFT and WT methods are illustrated in Figures 5 and 6. We can see that the energy of all the relative angular accelerations are mainly distributed in the frequency range below 4Hz and the decreasing tendencies in frequency band above 2Hz, between 6 to 12s, caused by the damages of the structure, are clearly presented. In Figure 4 the energy for each IMF is efficiently separated and the peaks of energy are distinctly located. It is also clear that the first 5 IMFs carry the majority of the signal energy. But in Figure 3, the energy of all the IMFs are blended with each other, and we cannot recognize the corresponding energy for each IMF from the Hilbert spectra. It can be concluded that Figure 4 exhibits better frequency resolution, localization of energy and tracking ability than Figure 3.

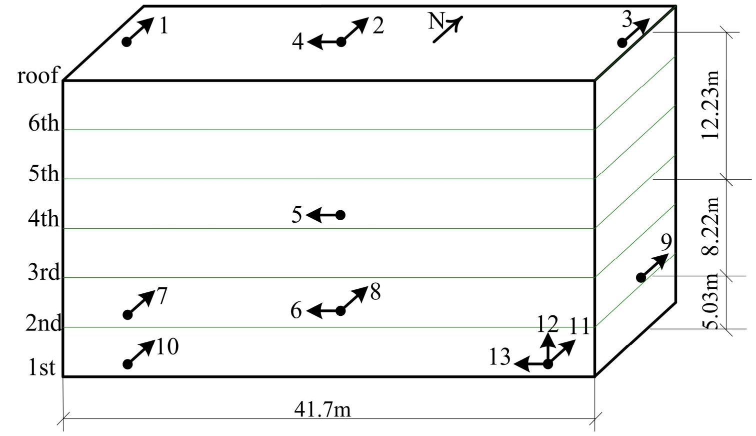

Figure 1 Sensor locations and orientations of the recording system

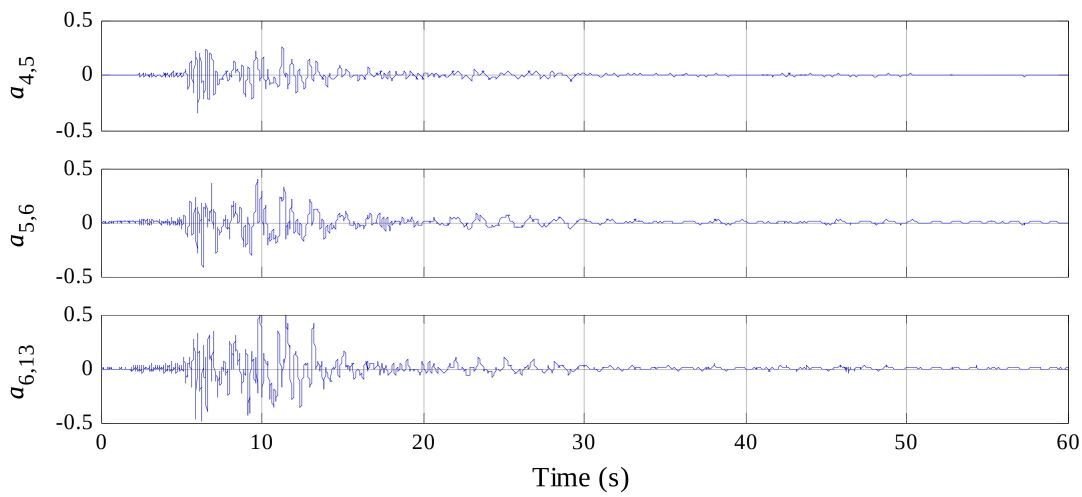

Figure 2 Relative angular accelerations in rads^{-2}

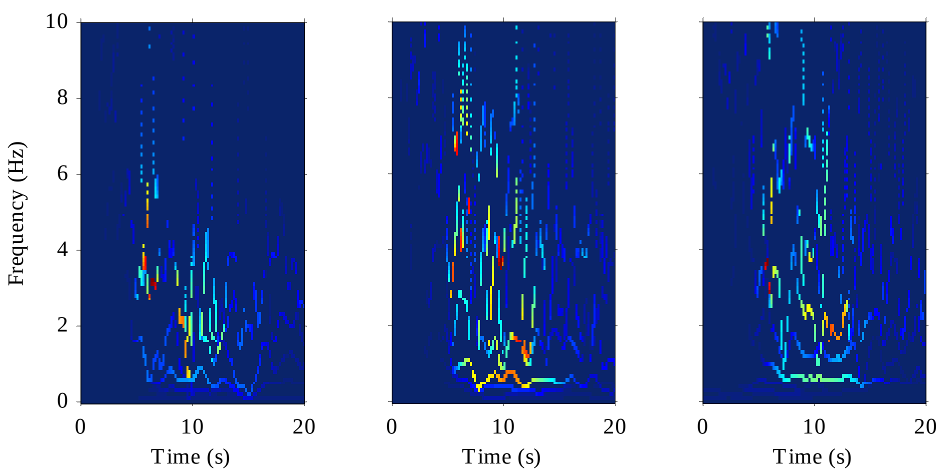

Figure 3 Hilbert spectra obtained by using the original HHT method

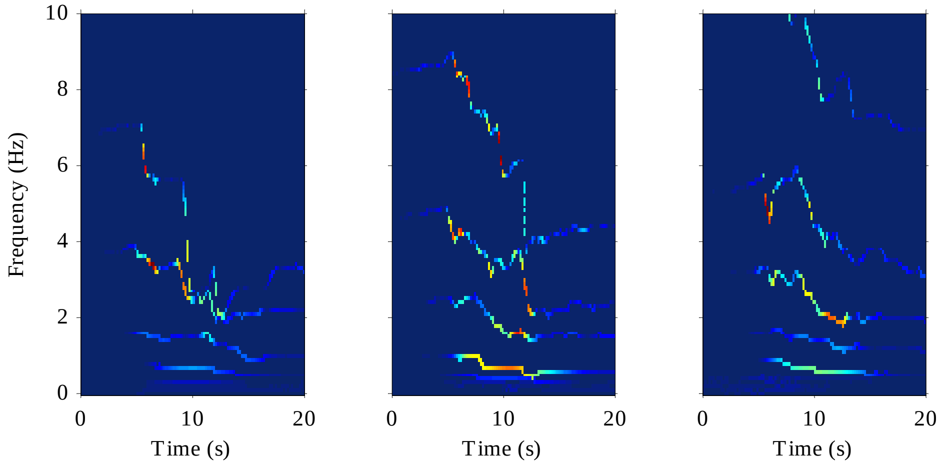

(a) $a_{4,5}$ (b) $a_{5,6}$ (c) $a_{6,13}$

Figure 4 Hilbert spectra obtained by using the improved HHT method

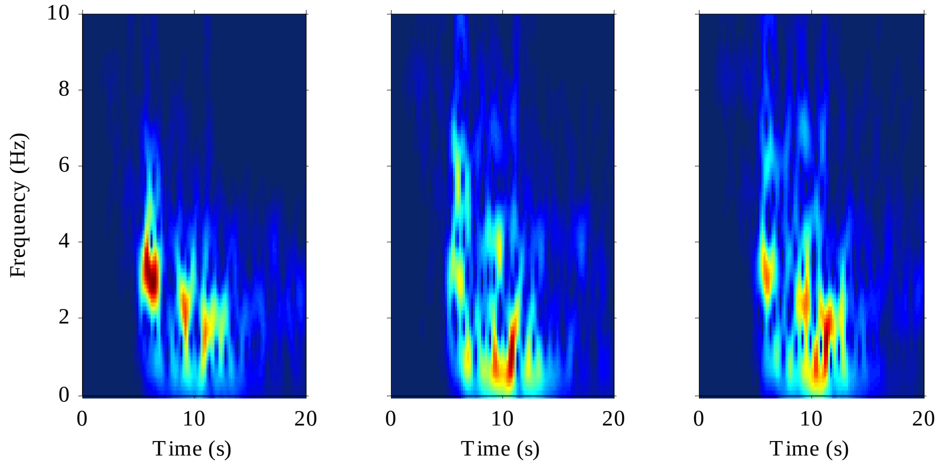

(a) $a_{4,5}$ (b) $a_{5,6}$ (c) $a_{6,13}$

Figure 5 Time varying spectra obtained by using the STFT method

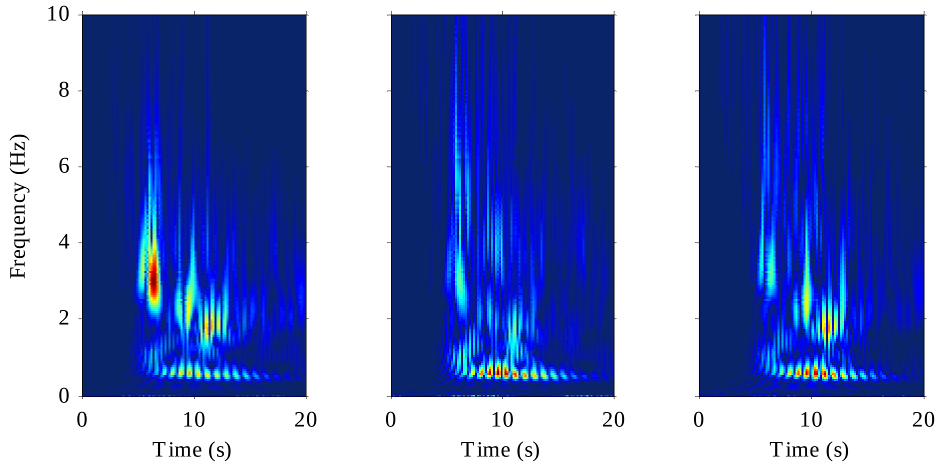

(a) $a_{4,5}$ (b) $a_{5,6}$ (c) $a_{6,13}$

Figure 6 Time varying spectra obtained by using the WT method

The time varying spectra in Figures 5 and 6 are somewhat smooth but their time and frequency resolution is obviously poorer than the Hilbert spectra which give much more details. Furthermore, comparing Figures 5 and 6 we can see in the frequency range below 2Hz the frequency resolution in Figure 6 is better, which is mainly because the filtering properties of the STFT and WT methods are quite different as discussed in the literature. For the STFT method, the effective length of time window is fixed, while for the WT method the effective length of time window is in direct proportion to the wavelet scales, i.e. it is shorter at higher frequencies (smaller scales) and longer at lower frequencies (larger scales).

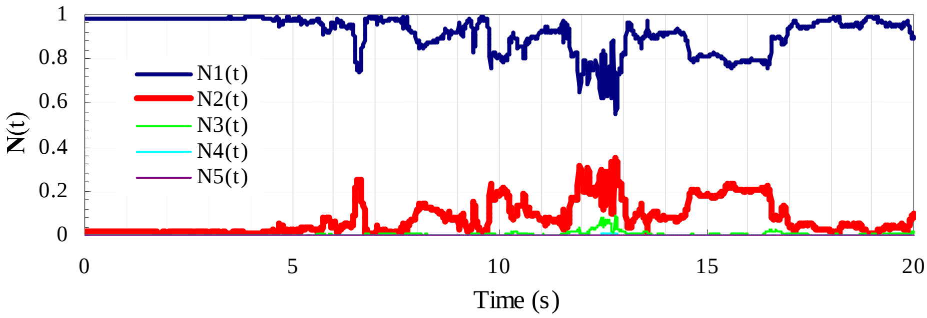

(a) $a_{4,5}$

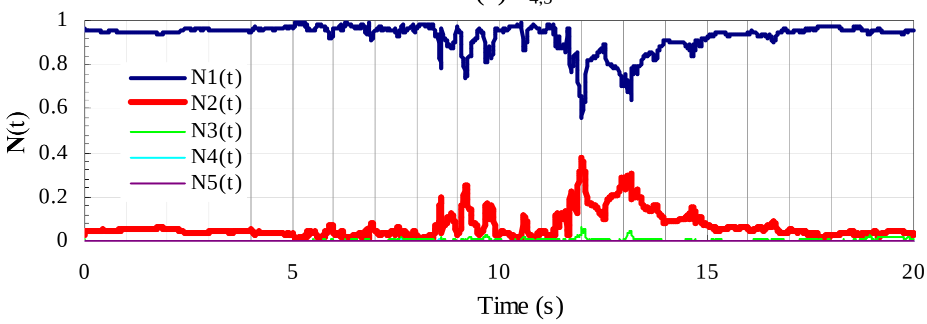

(b) $a_{5,6}$

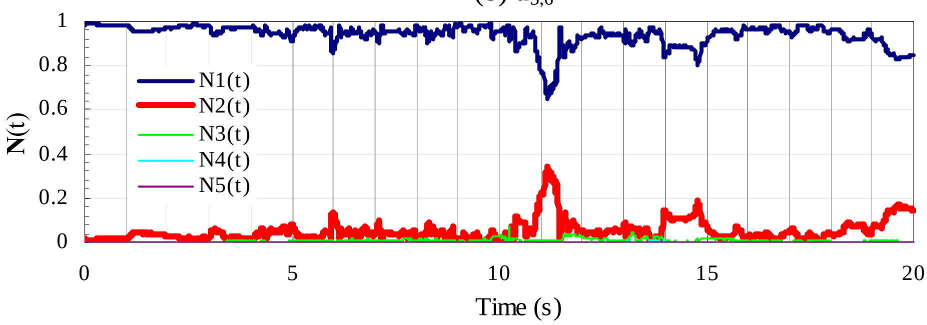

(c) $a_{6,13}$

Figure 7 Novelty indices corresponding to the relative angular accelerations

Figure 7 presents the novelty indices corresponding to relative angular accelerations in Figure 2. As has been mentioned above, the novelty index is designated to quantify the relative contribution of each IMF to the global energy distribution of response signal $x(t)$ in the high frequency band around $f_1(t)$, so we can see from Figure 7 that the novelty indices for the first 2 IMFs, i.e. $N_1(t)$ and $N_2(t)$, are predominant. Several abrupt changes (spikes) appear at about 6, 8, 10, 11, 12, 13 and 14s with $N_1(t)$ decreasing rapidly from about 0.95 to 0.7 and $N_2(t)$ increasing from about 0.05 to 0.3 simultaneously. These abrupt changes (spikes) clearly describe the damage process of the structure, i.e. at about 6 s damage first occurs and proceeds between 8 and 10s, culminated damage appears between 11 and 13s with the decrement of $N_1(t)$ and increment of $N_2(t)$ reaching their maxima, then minor damage occurs between 13 and 16s, and after 16s no further damage occurs. It can also be seen that in Figure 7(c) the culminated damage occurs at about 11s while in Figures 7(a) and (b) the culminated damage occurs at about at about 13 and 12s respectively, which indicates that the ground floor is damaged first and then the upper floors are damaged.

5. CONCLUSIONS

In this study, based on the improved HHT method by the author, a novelty index is proposed to detect the damage of structures. The basic idea of the approach is, similar to existing wavelet-based approaches, that the abrupt changes in high frequency part of response due to structural damage can be detected by novelty analysis. As the novelty index is defined based on the feature extraction of a signal and no additional modal information is required, it can be used to detect both global and local structural damages. Another merit of the novelty index is that it can be potentially used for real time (online) structural damage detection, for it is derived from time varying VARMA coefficients. In the example given, the Imperial County Services Building is used as testbed to explore the efficiency of the proposed novelty index. The results, which confirm the findings of other previous studies, demonstrate that the novelty index can indicate the occurrence and relative severity of structural damages at multiple locations in an efficient manner. It is also found that the improved HHT method can provide much exploitable information on time-frequency properties of structural responses for damage detection. Lastly, though the efficiency of the proposed novelty index has been validated by an example, the quantity relationship between the damage severity and the novelty index is still an important issue to be further studied and refined.

ACKNOWLEDGEMENTS

This work was supported by National Natural Science Foundation of China under Grant Nos. 50008017 and 50578167 and Program for New Century Excellent Talents in University (NCET-06-0765).

REFERENCES

Sohn, H., Farrar, C.R., Hemez, F.M., Shunk, D.D., Stinemates, D.W. and Nadler, B.R. (2003). A review of structural health monitoring literature: 1996-2001, LA-13976-MS, Los Alamos National Laboratory, USA.

Chang, P.C., Flatau, A. and Liu, S.C. (2003). Review paper: health monitoring of civil infrastructure. *Structural Health Monitoring* **2,** 257-67.

Huang, N.E., Shen, Z., Long, S.R., Wu, M.C., Shih, H.H., Zheng, Q., Yen, N.C., Tung, C.C. and Liu, H.H. (1998). The empirical mode decomposition and the Hilbert spectrum for nonlinear and non-stationary time series analysis. *Proceedings of R. Soc. London, Ser. A* **454,** 903-995.

Dong, Y.F., Li, Y.M., Xiao, M.K. and Lai, M. (2008). Analysis of earthquake ground motions using an improved Hilbert–Huang transform. *Soil Dynamics & Earthquake Engineering* **28:1,** 7-19.

Todorovska, M.I. and Trifunac, M.D. (2007). Earthquake damage detection in the Imperial County Services Building I: The data and time–frequency analysis. *Soil Dynamics & Earthquake Engineering* **27,** 564-576.

Todorovska, M.I. and Trifunac, M.D. (2008). Earthquake damage detection in the Imperial County Services Building III: Analysis of wave travel times via impulse response functions, *Soil Dynamics & Earthquake Engineering* **28,** 387-404.

Pandit, S.M. (1991). Modal and spectrum analysis: data dependent systems in state space, Wiley, New York.

Andersen, P. (1997). Identification of civil engineering structures using ARMA models, PhD Thesis, Aalborg University.

Ljung, L. (1999). System identification: theory for the user (2nd Edition), Prentice Hall, New York.

Dong, Y.F. and Li, Y.M. (2006). Application of time series analysis on performance evaluation of seismic structures. *Proceedings of the Ninth International Symposium on Structural Engineering for Young Experts* **1,** 820-826.

Flandrin, P., Rilling, G. and Goncalves, P. (2004). Empirical mode decomposition as a filter bank. *IEEE Signal Processing Letters* **11,** 112-114.